PROCEEDINGS OF SPIE

SPIEDigitalLibrary.org/conference-proceedings-of-spie

Modeling of operation regimes in coupled-cavity surface-emitting laser with external photon injection

Alrawashdeh, Medin M. A. , Lysenko, Hennadiy , Tuzhanskyi, Stanislav Ye., Abramchuk, Igor , Komada, Paweł, et al.

Medin M. A. Alrawashdeh, Hennadiy L. Lysenko, Stanislav Ye. Tuzhanskyi, Igor V. Abramchuk, Paweł Komada, Akmaral Tleshova, Gulzat Ziyatbekova, "Modeling of operation regimes in coupled-cavity surface-emitting laser with external photon injection," Proc. SPIE 11045, Optical Fibers and Their Applications 2018, 110450S (15 March 2019); doi: 10.1117/12.2522107

SPIE.

Event: 18th Conference on Optical Fibers and Their Applications, 2018, Naleczow, Poland

Modeling of operation regimes in coupled-cavity surface-emitting laser with external photon injection

Medin M. A. Alrawashdeh*[a], Hennadiy L. Lysenko[a], Stanislav Ye. Tuzhanskyi[a], Igor V. Abramchuk[a], Paweł Komada[b], Akmaral Tleshova[c], Gulzat Ziyatbekova[d]
[a]Vinnytsia National Technical University, 95 Khmelnytske shose, 21021,Vinnytsia, Ukraine; [b]Lublin University of Technology, 38A Nadbystrzycka Str., 20-618 Lublin, Poland; [c]Taraz State University after M.Kh.Dulaty, 7 Suleymenov Str., 080012, Taraz, Kazakhstan; [d]Al-Farabi Kazakh National University, 71 al-Farabi Str., 050040, Almaty, Kazakhstan

ABSTRACT

We present rate equation model of a modified vertical surface-emitting laser with two optical-coupled active cavities (CC-VSCEL) and external optical channel. The model allows to determine all the relevant parameters – carrier densities, gains, and output powers – starting from two input parameters: the injection currents in each cavity taking into account the additional external photonic injection. The system of rate equations is solved for different operating regimes of the modified laser device. The results provided by the model shown that operating characteristics of CC-VCSEL greatly depend on the number of photons of the external injection.

Keywords: coupled-cavity VCSELs, rate equation model, multisection device

1. INTRODUCTION

One of the limiting factors in the development of the photonic computing systems was the imperfection of diode laser emission. In vertical-cavity surface-emitting lasers (VCSEL) the symmetric optical beam with low divergence was obtained, single-mode generation regime with low threshold current and fast response (≥10Gbit/sec) is realized[1–4]. The technology of CC-VCSEL became the improvement of VCSEL, where optical bistability is realized, taking into account modes polarization in generation regime of two laser emission wavelengths[5–10]. Its implementation has good prospects for the creation of the planar structures with great number of individually and coupled addressable emitters CC-VCSEL. It enables to create 2D data arrays in the form of the beams of phase-coupled coherent polarized emission within specialized photon devices for matrix calculations[10–12].

2. AIM OF THE RESEARCH

In the given research, on the base of rate equations for the hypothetically modified structure of CC-VCSEL with the external photon injection, suggested in[11] simulation study of the characteristics of the device for operating stationary regimes with different input and output parameters of the model is performed, taking into consideration the impact of the amount of the external photons in the cavity and realized by means of computer algebra system Mathcad 15.

3. RATE EQUATION FOR CC-VCSEL WITH THE PHOTON INJECTION

We will consider the CC-VCSEL, formed by two optically coupled active cavities, scheme of which is suggested in[10,11]. The structure of CC-VCSEL with the hypothetical channel for the additional photon injection (for instance, for data transmission) is shown in Fig. 1[10]. Technological aspects of channel formation and the parameters of its emission we will leave aside the dissension in the given research[13–15].

*medin.mohamed@gmail.com

Optical Fibers and Their Applications 2018, edited by Ryszard S. Romaniuk, Waldemar Wójcik, Andrzej Smolarz, Proc. of SPIE Vol. 11045, 110450S

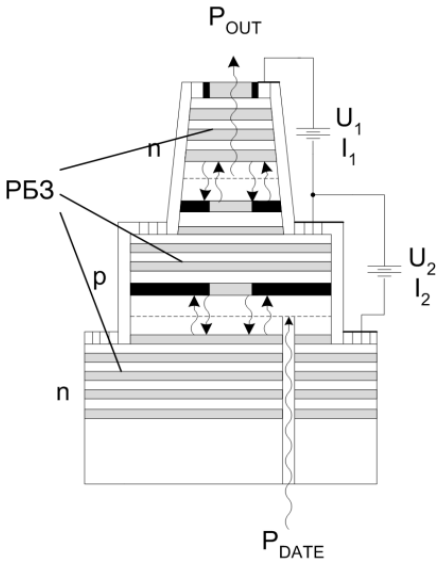

Figure 1. Structure of CC-VCSEL with the external photon injection

Rate equation CC-VCSEL were obtained on the base of the model of photon-reservoirs, suggested by V. Badilita and coauthors in[7,10,16]. The equations are modified for CC-VCSEL with the hypothetical external photon injection in[10,11,17].

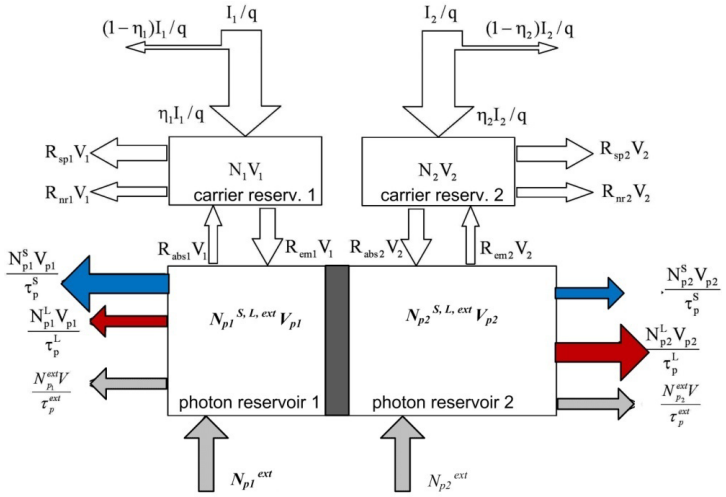

Figure 2. Model of the photon-reservoirs of CC-VSCEL with the external optical injection[10]

In the model of the photonic-reservoirs (Fig. 2), the limited volume V_i with a certain number of carriers N_i ($i = 1$ – top cavity, $i = 2$ – bottom cavity) is allocated to each of the structures zones, numbers of the photons in each mode are determined for the photon-reservoirs N_{pi}^{S} and N_{pi}^{L} (S – short, L – long mode), correspondingly. Designations in Fig. 2: I/q – carriers injection rate of the laser; η_i – carriers injection efficiency reaching the active region; $R_{nri}V_i$ – rate of non-radiative recombination; $R_{sp\,i}V_i$ – rate of spontaneous recombination. Additionally external optical wave with the number of photons $N_{p\,i}^{ext}$ in each photon reservoirs is present (we conventionally assume the number of external photons in each cavities to be equal: $N_{p\,1}^{ext} = N_{p\,2}^{ext} = N_{p}^{ext}$).

Rate equations for the carriers and photons for CC-VCSEL with external injection are written as follows[11]:

$$\frac{\eta_1 I_1}{q} = A_1^S \cdot N_p^S \cdot g_1^S + A_1^L \cdot N_p^L \cdot g_1^L + A_1^{ext} \cdot N_p^{ext} \cdot g_1^{ext} + \frac{N_1}{\tau_e}, \quad (1)$$

$$\frac{\eta_2 I_2}{q} = A_2^S \cdot N_p^S \cdot g_2^S + A_2^L \cdot N_p^L \cdot g_2^L + A_2^{ext} \cdot N_p^{ext} \cdot g_2^{ext} + \frac{N_2}{\tau_e}, \quad (2)$$

$$N_p^S \cdot \left(A_1^S \cdot g_1^S + A_2^S \cdot g_2^S - \frac{1}{\tau_p^S} \right) = 0, \quad (3)$$

$$N_p^L \cdot \left(A_1^L \cdot g_1^L + A_2^L \cdot g_2^L - \frac{1}{\tau_p^L} \right) = 0, \quad (4)$$

$$N_p^{ext} \cdot \left(A_1^{ext} \cdot g_1^{ext} + A_2^{ext} \cdot g_2^{ext} - \frac{1}{\tau_p^{ext}} \right) = 0, \quad (5)$$

where $g_i^{S,L,ext} = G_0^{S,L,ext} \cdot \ln \frac{n_i + n_0^{S,L,ext}}{n_{tr}^{S,L} + n_0^{S,L,ext}}$ – is the gain coefficient for the modes *S*, *L* and external mode in the cavity *i*, $n_i = N_i / V_i$ – is carrier density in the quantum wells, $n_{tr}^{S,L}$ – is the transparency carrier density in the cavity, which corresponds to zero gain, $n_0^{S,L,ext}$ determines the quantum well absorption at the corresponding wavelength; $A_i^{S,L} = 2\xi_i^{S,L} \frac{l_i}{L} \Gamma_i^{S,L}$, $A_i^{ext} = 2\xi_i^{ext} \nu^{ext} \Gamma_i^{\text{ext}}$ – are the constants containing the design parameters of the device. In this case $\nu_g^{S,L,ext}$ – is the group velocity of the photons in each of the modes, $V_{p,i}$ – is the volume of the photon reservoir *i*, $\xi_i^{S,L,ext}$ – is the standing wave enhancement factor (varies between 0 and 2, depending on the quantum wells in the field)[18–20].

Equation systems (1) – (5) contains seven unknown parameters: number of photons N_p^S, N_p^L and N_p^{ext}, number of carriers N_1 and N_2, injection currents I_1 and I_2. Having set any two of the seven parameters as „input parameters", the system of equations can be solved with the respect to the remaining five unknowns[21–23].

4. SIMULATION OF THE OPERATING REGIMES OF CC-VCSEL WITH THE PHOTON INJECTION

In the work[7,10] such operation regimes of CC-VSCEL device are considered (such regimes will be take place if the additional external photon channel is available):

A. The „double-threshold" point (point where both modes start lasing simultaneously);

B. The mode lasing threshold, if the other mode remains below thresholds value;

C. One mode lasing threshold if the order mode is above the threshold value;

D. One mode lasing far above the threshold value, if the value of other mode is below the threshold value;

E. Both modes have the values above the threshold.

For each of the above mentioned regimes the values of the corresponding injection currents must be interconnected to fulfill the lasing conditions. We will simulate the operation of our device in each of the regimes separately.

4.1 Case A. The „double-threshold" point

It is the point where lasing starts simultaneously for both modes, that is why the number of photons for each of the optic modes in the corresponding cavities 1 and 2 is zero: $N_p^S = 0$, $N_p^L = 0$.

The number of photons of the external emission N_p^{ext} is considered to be input parameter for modeling. The output parameters of the study we consider simulation dependences: $I_1\left(N_p^{ext}\right)$, $I_2\left(N_p^{ext}\right)$.

Taking into account the above-mentioned conditions the equations (1)-(5) can be writer in such form (for simplification we assume that the transparency carrier's density in the cavities is the same $n_{tr}^S = n_{tr}^L = n_{tr}$)[11]:

$$\frac{\eta_1 I_1}{q} = A_1^{ext} \cdot G_0^{ext} \cdot \ln\left(\frac{\frac{N_1}{V_1} + n_0^{ext}}{n_{tr} + n_0^{ext}}\right) \cdot N_p^{ext} + \frac{N_1}{\tau_e} \tag{6}$$

$$\frac{\eta_2 I_2}{q} = A_2^{ext} \cdot G_0^{ext} \cdot \ln\left(\frac{\frac{N_2}{V_2} + n_0^{ext}}{n_{tr} + n_0^{ext}}\right) \cdot N_p^{ext} + \frac{N_2}{\tau_e}, \tag{7}$$

$$A_1^S \cdot G_0^S \cdot \ln\left(\frac{\frac{N_1}{V_1} + n_0^S}{n_{tr} + n_0^S}\right) + A_2^S \cdot G_0^S \cdot \ln\left(\frac{\frac{N_2}{V_2} + n_0^S}{n_{tr} + n_0^S}\right) = \frac{1}{\tau_p^S}, \tag{8}$$

$$A_1^L \cdot G_0^L \cdot \ln\left(\frac{\frac{N_1}{V_1} + n_0^L}{n_{tr} + n_0^L}\right) + A_2^L \cdot G_0^L \cdot \ln\left(\frac{\frac{N_2}{V_2} + n_0^L}{n_{tr} + n_0^L}\right) = \frac{1}{\tau_p^L}, \tag{9}$$

$$A_1^{ext} \cdot G_0^{ext} \cdot \ln\left(\frac{\frac{N_1}{V_1} + n_0^{ext}}{n_{tr} + n_0^{ext}}\right) + A_2^{ext} \cdot G_0^{ext} \cdot \ln\left(\frac{\frac{N_2}{V_2} + n_0^{ext}}{n_{tr} + n_0^{ext}}\right) = \frac{1}{\tau_p^{ext}}. \tag{10}$$

We will introduce the following designations: $\nu_{\log i}^{S,L} = \ln\left(\frac{\frac{N_{i,0}}{V_i} + n_0^{S,L}}{n_{tr} + n_0^{S,L}}\right)$, $\nu_{\log i}^{ext} = \ln\left(\frac{\frac{N_{i,0}}{V_i} + n_0^{ext}}{n_{tr} + n_0^{ext}}\right)$.

Solving the system of equations (8)-(9) as the linear system, we obtain the expression for the number of carriers in double-threshold point $N_{i,0}$ in each of the cavities:

$$N_{i,0}^{S,L} = \left[\left(n_{tr}^{S,L} + n_0^{S,L}\right)\exp\left(\nu_{\log i}^{S,L}\right) - n_0^{S,L}\right]V_i \ . \tag{11}$$

Using same input parameters for simulation as the authors in[10] (Table 1), such values for the number of carriers and their density in double-threshold point for S – mode lasing

$$\nu_{\log i}^{ext} = \begin{pmatrix} 0,083 \\ 0,071 \end{pmatrix}, \quad \begin{pmatrix} N_{1,0} \\ N_{2,0} \end{pmatrix} = \begin{Bmatrix} 8,314 \cdot 10^6 \\ 3,966 \cdot 10^6 \end{Bmatrix}, \quad \begin{pmatrix} n_{1,0}^S \\ n_{2,0}^S \end{pmatrix} = \begin{Bmatrix} 2,598 \cdot 10^{18} \\ 2,479 \cdot 10^{18} \end{Bmatrix} cm^{-1}.$$

Density of the photons of the external injection n_0^{ext}, at which the conditions of the double-threshold point are satisfied, we determined further from the expression (10), substituting in it instead of N_1 and N_2 the values of the numbers of carriers , obtained above for S – mode $N_{1,0}$ and $N_{2,0}$: $n_0^{ext} = 7,3645 \cdot 10^{18} cm^{-1}$.

Table1. Input parameters of CC-VCSEL for modeling

Parameter	Physical quantities	Value
Standing wave enhancement factor	ξ_1^S , ξ_1^L , ξ_1^{ext}	1,63
	ξ_2^S , ξ_2^L , ξ_2^{ext}	1,92
Confinement coefficient	Γ_1^S, Γ_2^L	0,76
	Γ_1^S, Γ_2^L	0,24
	Γ_1^{ext}	0,4
	Γ_2^{ext}	0,6
Gain coefficient (cm^{-1})	G_0^S , G_0^{ext}	1800
	G_0^L	2000
Volume of the cavity (m^3)	V_1 V_2	$3{,}2\cdot10^{-12}$ $1{,}6\cdot10^{-12}$
Group velocity (m/s)	v_g^S , v_g^L , v_g^{ext}	$7{,}894\cdot10^{9}$
Photon lifetime (ps)	τ_p^S	0,289
	τ_p^L , τ_p^{ext}	0,257
Carrier escape time (ps)	τ^e	1
Carriers injection efficiency	η_1 , η_2	0,8
Carriers density in the quantum wells (cm^{-1})	n_0^S , n_0^L n_0^{ext}	$0{,}4\cdot10^{18}$
Transparency carrier density (cm^{-1})	n_{tr}^S , n_{tr}^L	$1{,}8\cdot10^{18}$
Cavity width (cm)	l_1 , l_2	$0{,}24\cdot10^{-4}$

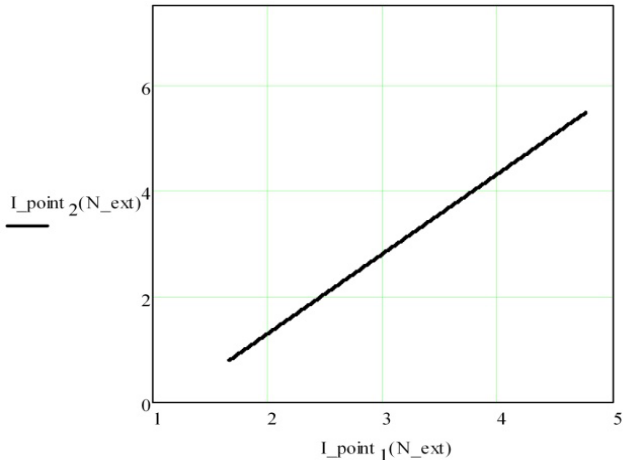

Figure 3. Dependence of the double-threshold point of CC-VCSEL on the injection currents (*mA*) if $N_p^{ext} = 0 \ldots 10^7$

Further, taking into account the obtained values $N_{1,0}$ and $N_{2,0}$, we solve the system of linear equations (6)-(7) respectively injection currents of the double-threshold point as the function from the number of the photons N_p^{ext} of the external injection for each of the cavities for *S* – mode:

$$I_{point\,1}(N_p^{ext}) = \frac{q}{\eta_1}(A_1^{ext} \cdot G_0^{ext} \cdot v_{\log_1}^{ext} \cdot N_p^{ext} + \frac{N_{1,0}}{\tau_e}),$$
$$I_{point\,2}(N_p^{ext}) = \frac{q}{\eta_2}(A_2^{ext} \cdot G_0^{ext} \cdot v_{\log_2}^{ext} \cdot N_p^{ext} + \frac{N_{2,0}}{\tau_e}) \quad (12)$$

The analysis of the resent studies shows that the position of the „double-threshold" point depends on the number of the external photons linearly. Its position on the directed line is determined from the expression (Fig. 3):

$$I_{point\,2} = k_x I_{point\,1} + k_y = \frac{\eta_1}{\eta_2}\frac{A_2^{ext}\cdot\nu_{\log_2}^{ext}}{A_1^{ext}\cdot\nu_{\log_1}^{ext}} I_{point\,1} + const\ . \tag{13}$$

Taking into consideration the parameters of model $k_x = 1{,}512$. The results of the simulation for L-mode are analogous.

4.2 Case B. Borders of the „one-mode lasing" regions

In this regime the lasing conditions for one of the modes are not valid (since its value is under threshold values).

East we simulate the operation of L-mode for the case, when the value of S-mode is under the threshold values. In the system of rate equations, taking into account the external photon injection the equation (8) is not valid[24].

As the output, thus in *Case A*, we have $N_p^S = N_p^L = 0$.

We will simulated the dependence $I_2\left(I_1, N_p^{ext}\right)$.

In this case the equation (9) can be written

$$N_2(N_1) = \left[(n_{tr} + n_0^L) \exp\left(\frac{-A_1^L}{A_2^L} \ln\left(\frac{\frac{N_1}{V_1} + n_0^L}{n_{tr} + n_0^L} \right) + \frac{1}{A_2^L \tau_p^L G_0^L} \right) - n_0^L \right] V_2\,. \tag{14}$$

The solution of the non-linear equation (6) will be done in Mathcad 15 package using the Lambert is *W*-function. After a set of mathematical transformations we obtain the dependence of the number of carriers in the second cavity on the injection current in the first cavity and a number of the external photons for the *L*-mode:

$$N_2^L(I_1, N_p^{ext}) = \left[(n_{tr} + n_0^L) \exp\left(\frac{-A_1^L}{A_2^L} \ln\left(\frac{\frac{N_{1B}(I_1, N_p^{ext})}{V_1} + n_0^L}{n_{tr} + n_0^L} \right) + \frac{1}{A_2^L \tau_p^L G_0^L} \right) - n_0^L \right] V_2\,, \tag{15}$$

where

$$N_{1B}(I_1, N_p^{ext}) = V_1 \left[(n_{tr} + n_0^L) \left(\frac{1}{\beta(N_p^{ext})} \mathrm{W}\left[\beta(N_p^{ext}) e^{\alpha(I_1, N_p^{ext})} \right] \right) - n_0^{ext} \right];$$

$$\beta(N_p^{ext}) = \frac{V_1 (n_{tr} + n_0^{ext})}{A_1^{ext} \tau_e G_0^{ext} N_p^{ext}};$$

$$\alpha(I_1, N_p^{ext}) = \frac{1}{A_1^{ext} G_0^{ext} N_p^{ext}} \left(\frac{\eta_1}{q} I_1 + \frac{n_0^{ext} V_1}{\tau_e} \right).$$

Substituting (15) into (7) we obtain the expression of the target output dependence for *L*-mode

$$I_{2B}^L(I_1, N_p^{ext}) = \frac{q}{\eta_2} \left[A_2^{ext} G_0^{ext} N_p^{ext} \ln\left(\frac{\frac{N_2^L(I_1, N_p^{ext})}{V_2} + n_0^{ext}}{n_{tr} + n_0^{ext}} \right) + \frac{N_2^L(I_1, N_p^{ext})}{\tau_e} \right] \tag{16}$$

In the same way we obtain the output dependence for S-mode in the regime, if L-mode is below the threshold (in the system of rate equation the equation (7) is not valid).

The expression of the target output dependence for S-mode (L-mode is under the threshold):

$$I_{2B}^{S}(I_1, N_p^{ext}) = \frac{q}{\eta_2}\left[A_2^{ext} G_0^{ext} N_p^{ext} \ln\left(\frac{\frac{N_2^S(I_1, N_p^{ext})}{V_2} + n_0^{ext}}{n_{tr} + n_0^{ext}} \right) + \frac{N_2^S(I_1, N_p^{ext})}{\tau_e} \right] \tag{17}$$

Graphs in Fig. 4 illustrate the obtained dependences for each of mutually exclusive in the given regime *S* and *L* modes, taking into account the imposer constraints at the external injection of photons in the range of $N_p^{ext} = 1 \cdot 10^1 .. 5 \cdot 10^5$.

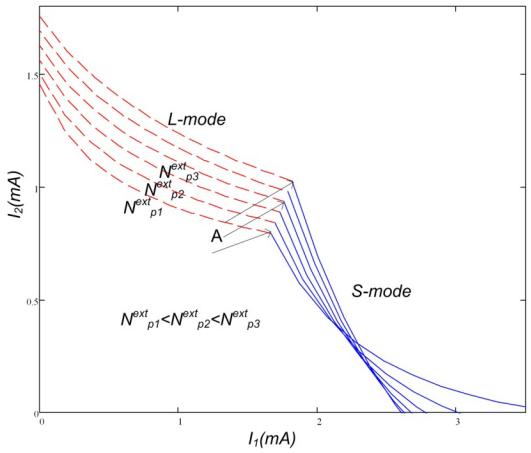

Figure 4. Calculated dependences of the threshold point on the injection currents for *Case B* if $N_p^{ext} = 1 \cdot 10^1 .. 5 \cdot 10^5$

4.3 Case C. Borders of the „both modes lasing" regions

In this mode two variants of the operation are possible:

1. Lasing of *S*- mode at the threshold of *L*-mode ($N_p^L = 0$ and $N_p^S > 0$);

2. Lasing of *L*- mode at the threshold of *S*-mode ($N_p^S = 0$ and $N_p^L > 0$).

In each of the variants the corresponding output characteristic is simulated $I_2\left(I_1, N_p^{ext}\right)$.

We will consider the first variant of the operation.

The solutions of the system of rate equations (3)-(4) for this case by analogy with *Case A* have the form (12). The solution of the system of linear equations (1)-(2) for *S*–mode in this case has the form:

$$I_{2C}{}^{S}\left(I_1, N_p^{ext}\right) = \frac{\eta_1}{\eta_2}\frac{A_2^S \nu_{\log 2}^S}{A_1^S \nu_{\log 1}^S}\left[I_1 - \frac{q}{\eta_1}\left(\frac{N_{1,0}}{\tau_e} + A_1^{ext} G_0^{ext} \nu_{\log 1}^{ext} N_p^{ext} \right) \right] + \frac{q}{\eta_2}\left(\frac{N_{2,0}}{\tau_e} + A_2^{ext} G_0^{ext} \nu_{\log 2}^{ext} N_p^{ext} \right). \tag{18}$$

The analysis of the formula shows that this function for *S*–mode changes linearly from the number of the external photons with the constant angular factor (for the parameters, set in the model it equals 3,241).

For the second variant (lasing of *L*-mode) the solution is found analogous:

$$I_{2C}{}^{L}\left(I_1, N_p^{ext}\right) = \frac{\eta_1}{\eta_2}\frac{A_2^L \nu_{\log 2}^L}{A_1^L \nu_{\log 1}^L}\left[I_1 - \frac{q}{\eta_1}\left(\frac{N_{1,0}}{\tau_e} + A_1^{ext} G_0^{ext} \nu_{\log 1}^{ext} N_p^{ext} \right) \right] + \frac{q}{\eta_2}\left(\frac{N_{2,0}}{\tau_e} + A_2^{ext} G_0^{ext} \nu_{\log 2}^{ext} N_p^{ext} \right). \tag{19}$$

Similarly, this function for *L*–mode changes linearly from the number of external photons with the constant angular factor (for the parameters, set in the model it equals 0,323).

Analyzing the obtained solutions we make the conclusions that:

1. Position of the „double-threshold" point depending on the number N_p^{ext} changes linearly,

2. Threshold values of modes *S* and *L* lasing are linearly.

Calculated dependences of the functions (18) and (19) on injection currents under the emission of the external photons in the range of values $N_p^{ext} = 1 \cdot 10^5 .. 9 \cdot 10^6$ are shown in Fig. 5.

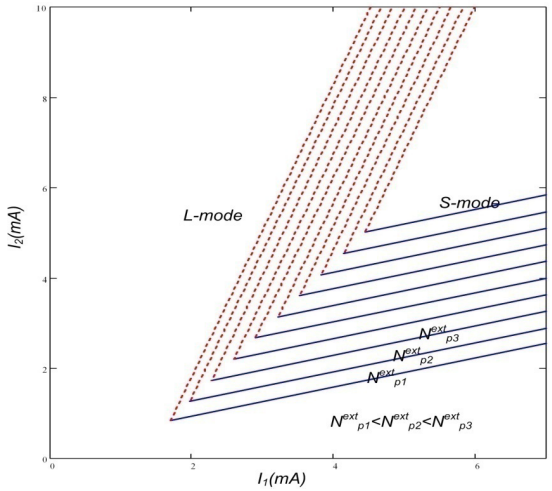

Figure 5. Calculation dependences of the injection currents functions in the cavities for the injection of the external photons in the range of $N_p^{ext} = 1 \cdot 10^5 .. 9 \cdot 10^6$

4.4 Case D. Inside the one-mode lasing regions

The solution of rate equations for CC-VSCEL with the account of the external photons injection in this regime using the Lambert's *W*-function is not possible (only by the numerical methods).

4.5 Case E. Inside the dual-mode lasing regions

Within the range of this operation regime two variants are considered:

1. $N_p^L = const$, $N_p^S > 0$,

2. $N_p^S = const$ and $N_p^L > 0$.

We will consider $I_2\left(I_2, N_p^{ext}, N_p^L\right)$ and $I_2\left(I_2, N_p^{ext}, N_p^S\right)$ as the output characteristic, correspondingly.

The solution of the equations (3)-(4) is considered in *Case A, C*. By analogy, the following dependences are obtained for variant 1:

$$I_{2E}{}^S\left(I_1, N_p^{ext}, N_p^L\right) = \frac{\eta_1}{\eta_2}\frac{A_2^S v_{\log 2}^S}{A_1^S v_{\log 1}^S}\left[I_1 - \Delta I_1^S(N_p^{ext}, N_p^L) + \Delta I_2^S(N_p^{ext}, N_p^L)\right], \tag{20}$$

where:

$$\Delta I_1^S(N_p^{ext}, N_p^L) = \frac{q}{\eta_1}\left(\frac{N_{1,0}}{\tau_e} + A_1^{ext} G_0^{ext} v_{\log 1}^{ext} N_p^{ext} + A_1^L G_0^L v_{\log 1}^L N_p^L\right),$$

$$\Delta I_2^S(N_p^{ext}, N_p^L) = \frac{q}{\eta_1}\left(\frac{N_{2,0}}{\tau_e} + A_2^{ext} G_0^{ext} \nu_{\log 2}^{ext} N_p^{ext} + A_2^L G_0^L \nu_{\log 2}^L N_p^L\right).$$

For variant 2 the analogous (20) expressions are obtained:

$$I_{2E}{}^L\left(I_1, N_p^{ext}, N_p^S\right) = \frac{\eta_1}{\eta_2}\frac{A_2^L \nu_{\log 2}^L}{A_1^L \nu_{\log 1}^L}\left[I_1 - \Delta I_1^L(N_p^{ext}, N_p^S) + \Delta I_2^L(N_p^{ext}, N_p^S)\right], \tag{21}$$

where

$$\Delta I_1^L(N_p^{ext}, N_p^S) = \frac{q}{\eta_1}\left(\frac{N_{1,0}}{\tau_e} + A_1^{ext} G_0^{ext} \nu_{\log 1}^{ext} N_p^{ext} + A_1^S G_0^S \nu_{\log 1}^S N_p^S\right),$$

$$\Delta I_2^L(N_p^{ext}, N_p^S) = \frac{q}{\eta_1}\left(\frac{N_{2,0}}{\tau_e} + A_2^{ext} G_0^{ext} \nu_{\log 2}^{ext} N_p^{ext} + A_2^S G_0^S \nu_{\log 2}^S N_p^S\right).$$

Fig. 6 shows the calculations dependences of lasing threshold point for all the regimes taking into account *Case E* (excluding *Case D*) at $N_p^{ext} = 10^4$, $N_p^S = N_p^L = 10^6$.

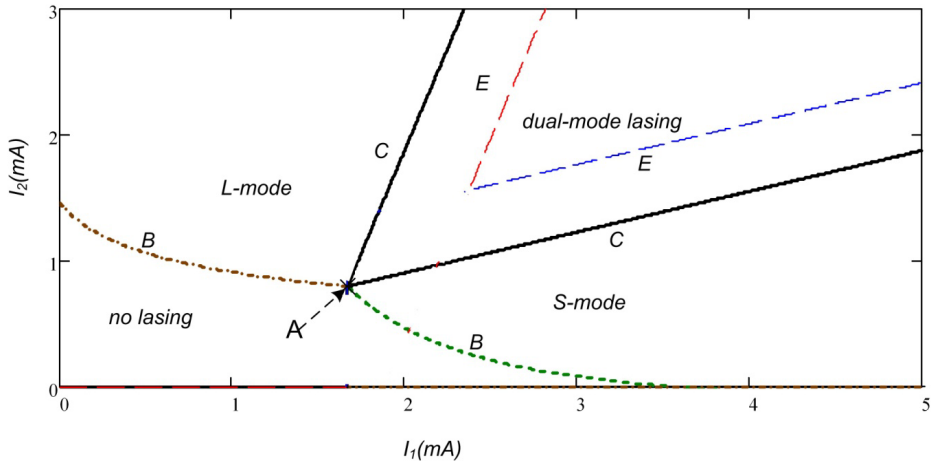

Figure 6. Calculation dependences of CC-VSCEL injection currents with the external photon injection, taking into account the thresholds for *Cases A, B, C, E* at $N_p^{ext} = 10^4$, $N_p^S = N_p^L = 10^6$

Graphs in Fig. 6 illustrate the obtained dependences for *S* and *L* modes in regimes *A, B, C, E* of CC-VCSEL operation, taking into account the parameters of the model (Table 1).

5. CONCLUSIONS

In the process of the investigation of operating regimes of CC-VCSEL with additional external photon injection in the cavity, it is shown that operating characteristics in the considered cases in stationary conditions greatly depend on the number of photons of the external injection. The analysis of the obtained analytical solutions allowed to make or conclusion regarding the character of the obtained dependences in basic working regimes of the laser multisection device. The results of the simulation can be useful for the development of basic modules of specialized photon systems for matrix computation[9,11].

REFERENCES

[1] Koyama, F., "Recent Advances of VCSEL Photonics," J. Lightwave Technol. 24, 4502-4513 (2006).
[2] Brunner, M., Gulden, K., Hovel, R., Moser, M., Carlin, J.-F., Stanley, R. P. and Ilegems M., "Continuous-wave dual-wavelength lasing in a two-section vertical-cavity laser," IEEE Photon. Technol. Lett. 12, 1316-1325 (2000).
[3] Nakwaski, W. and Sarzała, R., ″Semiconductor lasers,″ Przegląd Elektrotechniczny 91(9), 147-149 (2015).
[4] Sarzała, R. and Nakwaski, W., ″The beginnings and development of VCSELs,″ Przegląd Elektrotechniczny 93(8), 1-8 (2017).
[5] Wójcik-Jedlińska, A., Broda, A., Muszalski, J., Szerling, A., Bugajski, M., Gębski, M. and Czyszanowski, T., ″Innovative architectures of verticalcavity surface-emitting lasers,″ Przegląd Elektrotechniczny 93(8), 85-88 (2017).
[6] Leinonen, T., Morozov, Yu. A., Härkönen, A., and Pessa, M., "Vertical external-cavity surface-emitting laser for dual-wavelength generation," IEEE Photon. Technol. Lett. 17, 2508-2510 (2005).
[7] Badilita, V., Carlin, J.-F., Brunner, M. and Ilegems, M., "Light-current characterization of dual-wavelength VCSELs," Proc. SPIE 4649, 87-95 (2002).
[8] Grasso, D. M. and Choquette, K. D., "Threshold and modal characteristics of composite-resonator vertical-cavity lasers," IEEE Journal of Quantum Electronics 39(12), 1526-1530 (2003).
[9] Zujewski, M., Thienpont, H. and Panajotov, K., "Traveling wave electro-optically modulated coupled-cavity surface emitting lasers," Proc. SPIE 8639, 3901-3912 (2013).
[10] Badilita, V., Carlin, J.-F., Ilegems, M. and Panajotov, K., "Rate-equation model for coupled-cavity surface-emitting lasers", IEEE J. Quantum Electron. 40, 1646-1656 (2004).
[11] Lysenko, H., Tuzhanskyi, S. and Alrawashdeh, M. "Optoelectronic adder-multiplier for realization of the DMAC algoritm," Optoelectronic Information-Power Technologies 32(2), 43-56 (2017).
[12] Badilita, V., Carlin, J.F., Ilegems, M., Brunner, M.J., Verschaffelt, G. and Panajotov, K., "Control of polarization switching in vertical coupled-cavities surface emitting lasers, " IEEE Photonics Technology Letters 16, 365-367 (2004).
[13] Kolobrodov, V. G. and Tymchyk, G. S., [Applied Diffractive Optics], NTUU KPI, Kiev (2014).
[14] Kolobrodov, V. G. Tymchik, G. S., Mykytenko, V. I., Kolobrodov, M. S. and Lutsiuk, M. M., "Influence of the matrix structure of the modulator and detector on the output signal of the optical spectrum analyzer," Visnyk NTUU KPI – Radiotekhnika Radioaparatobuduvannia 72, 78-85 (2018).
[15] Lloyd, J.M., [Thermal Imaging Systems], Mir, Moscow (1978).
[16] Wójcik, W., Smolarz. A., [Information Technology in Medical Diagnostics], Taylor &Francis Group CRC Press, London (2018).
[17] Pavlov, S. V., Kozhemiako, V. P., Kolesnik, P. F., et al., [Physical principles of biomedical optics], VNTU, Vinnytsya (2010).
[18] Pavlov, S. V., Tuzhanskyy, S. E., Kozlovska T. I. and Kozak, A. V., "A simulation model of distribution of optical radiation in biological tissues," Visnyk VNTU 3, 191-195 (2011).
[19] Kholin, V. V., Chepurna, O. M., Pavlov, S., et al., "Methods and fiber optics spectrometry system for control of photosensitizer in tissue during photodynamic therapy," Proc. SPIE 10031, 1003138 (2016).
[20] Rovira, R. H., Tuzhanskyy, S. Ye., Pavlov, S. V., et al., "Polarimetric characterisation of histological section of skin with pathological changes," Proc. SPIE 10031, 100313E (2016).
[21] Pavlov, S. V., Vassilenko, V. B., et al., "Methods of processing biomedical image of retinal macular region of the eye," Proc. SPIE 9961, 99610X (2016).
[22] Rovira, R., Bayas, M. M., Pavlov, S. V., Kozlovskaya, T. I., Kisała, P., et al. "Application of a modified evolutionary algorithm for the optimization of data acquisition to improve the accuracy of a video-polarimetric system," Proc. SPIE 9816, 981619 (2015).
[23] Zabolotna, N. I., Pavlov, S. V., Radchenko, K. O., Stasenko, V. A., Wójcik, W., et al. "Diagnostic efficiency of Mueller-matrix polarization reconstruction system of the phase structure of liver tissue," Proc. SPIE 9816, 98161E (2015).
[24] Zabolotna, N. I., Pavlov, S. V., Ushenko, A. G., Sobko, O. V. and Savich, V. O., "Multivariate system of polarization tomography of biological crystals birefringence networks," Proc. SPIE 9166, 916615 (2014).